flows, seems to support the speculation[8] that temperature fluctuations show larger departures from local isotropy than velocity fluctuations.

Cospectral values for the combinations u-v, v-θ, and also u-θ are shown in Fig. 3 for $x/d=40$ and for $\eta \simeq 0.5$. The cospectrum Co is defined such that the area under the distributions is equal to the correlation coefficient $\rho_{\alpha\beta}$ ($\equiv \overline{\alpha\beta} / \overline{\alpha^2}^{1/2}\,\overline{\beta^2}^{1/2}$, where α, β stand for u, v, or θ). All three cospectra exhibit a maximum at approximately the same frequency ($\ell n\omega^* \simeq -0.2$). For frequencies smaller than this peak frequency, Co_{uv} is larger than $Co_{v\theta}$ whereas $Co_{v\theta}$ is slightly larger than Co_{uv} at higher frequencies. This trend is in reasonable agreement with that previously reported for other flows but there is practically no difference (Fig. 3) between the coherences Coh_{uv} and $Coh_{v\theta}$ [note, $Coh_{\alpha\beta} = (Co^2 + Q^2)/(F_\alpha F_\beta)$, where Q is the quadrature spectrum] for frequencies greater than that at which the cospectra are maximum.

Conclusions

The analogy between F_θ and F_q, introduced and verified for the case of a slightly heated turbulent boundary layer,[1] applies to the self-preserving region of a turbulent plane jet. In this region, the spectrum of v differs from other velocity spectra but this difference, especially near the jet centerline, is much less marked than in the boundary layer.[2] In the jet, the cospectra and, in particular, the coherences between longitudinal and lateral velocity fluctuations do not differ appreciably from those between temperature and the lateral velocity fluctuations. This difference is much more pronounced in the boundary layer.[1] In this latter flow, a close liaison is maintained, close to the heated wall, between F_u and F_θ. The temperature spectrum becomes progressively more dependent on the spectrum of v as the distance from the wall increases. In the jet, the temperature spectrum depends on all three velocity fluctuations, especially near the centerline.

Acknowledgment

The first author is grateful for the support of the Australian Research Grants Scheme.

References

[1] Fulachier, L. and Dumas, R., "Spectral Analogy Between Temperature and Velocity Fluctuations in a Turbulent Boundary Layer," *Journal of Fluid Mechanics*, Vol. 77, Sept. 1976, pp. 257-277.

[2] Fulachier, L., "Contribution a l'Etude des Analogies des Champs Dynamique et Thermique dans une Couche Limite Turbulente. Effet de l'Aspiration," These de Docteur es Sciences Physiques, Université de Provence, 1972.

[3] Fulachier, L., "Spectral Analogy Between Temperature and Velocity Fluctuations in Various Turbulent Flows," AIAA Paper presented at AIAA/ASME Thermophysics and Heat Transfer Conference: Fundamentals of Turbulent Heat Transport Processes, Palo Alto, Calif., 1978.

[4] Corrsin, S., "Remarks on Turbulent Heat Transfer," *Proceedings of the Iowa Thermodynamics Symposium*, State University of Iowa, Iowa City, Iowa, 1953.

[5] Antonia, R. A., Browne, L.W.B., Chambers, A. J., and Rajagopalan, S., "Budget of the Temperature Variance in a Turbulent Plane Jet," *International Journal of Heat and Mass Transfer*, Vol. 26, No. 1, 1983, pp. 41-48.

[6] Cervantes de Gortari, J. and Goldschmidt, V. W., "The Apparent Flapping Motion of a Turbulent Plane Jet—Further Experimental Results," *Journal of Fluids Engineering*, Vol. 103, May 1981, pp. 119-126.

[7] Chevray, R. and Tutu, N. K., "Intermittency and Preferential Transport of Heat in a Round Jet," *Journal of Fluid Mechanics*, Vol. 88, Sept. 1978, pp. 133-160.

[8] Tavoularis, S. and Corrsin, S., "Experiments in Nearly Homogeneous Turbulent Shear Flow with a Uniform Mean Temperature Gradient. Part 2. The Fine Structure," *Journal of Fluid Mechanics*, Vol. 104, March 1981, pp. 349-367.

Chemistry of Combustion of Double-Base Propellants Through Sliver Analysis

K. Kishore* and V. R. Pai Verneker†
Indian Institute of Science,
Bangalore, India
and
C.B.V. Subhas‡
Defence Research and Development
Laboratory, Hyderabad, India

Introduction

INTEREST in systematic study to understand the combustion mechanism of double-base propellants (DBP), thrives because the existing literature is inadequate to explain many experimental observations. Some detailed investigations on the combustion mechanism of composite propellants have been carried out in recent years in which attempts were made to understand the condensed-phase combustion mechanism through intermediary analysis.[1,2] The result strongly supports the occurrence of exothermic condensed-phase reactions.

In the present investigation an attempt has been made to show evidence of the occurrence and nature of condensed-phase reactions during combustion in double-base propellants through sliver analysis. The sliver sample is the self-extinguished propellant sample obtained from the actual motor firing. It is the belief that some clarification of the decomposition process in the surface layer of burning propellants can be made by examination of the surface material from the quenched samples.

The in situ burning surface (sliver sample) was obtained by natural flame extinguishment. The procedure is outlined in the next section. In the present work it is assumed that the sliver represents the true burning surface. It is believed that the analysis of this sliver sample will reveal the nature of chemical reactions occurring during the combustion of DBPs.

Experimental Procedure

The composition of the DBP used was: 26.5% nitroglycerine (NG), 57.5% nitrocellulose (NC), 5.0% dibutylphthalate, 6.0% dinitrotoluene (DNT)/trinitrotoluene (TNT), and 3.5% 2-nitrodiphenyl amine (2-nDPA) and the rest inorganic salts.

A 30 ton thrust motor was filled with 14 tubular uninhibited DBP propellant grains that burned from inside to outside as well as outside to inside. Setting the nozzle to a required pressure (70 kg·cm^{-2}), the motor was fired to evaluate the ballistic parameters. As the propellant burns, the web thickness decreases and contracts to such an extent that under the pressure the grain crumbles and the unburned pieces are thrown out. As the pieces come out of the nozzle, the burning stops because of a sudden drop in pressure. The pieces thus ejected from the motor (technically called as "slivers") were collected. The top layer (50 μm) of the sliver surfaces was scratched gently with a jewelery file to collect a dark brownish residue for analysis.

Received Aug. 13, 1982; revision received Feb. 2, 1983.

*Associate Professor, Department of Inorganic and Physical Chemistry.

†Professor, Department of Inorganic and Physical Chemistry.

‡Scientific Assistant, Solid Propellant Division.

The sliver residue was dissolved in chloromethane. The soluble portion was removed and concentrated. The sliver aliquot was analyzed by thin layer chromatography (TLC). Adjacent to the sliver sample, authentic samples of NG, TNT, and DNT were also placed on the TCL plate. The plate was developed with a benzene-petroleum ether-ethylacetate (12:12:1) eluent system. The plate was dried and subjected to spot test analysis using various reagents. With the Greiss reagent, one of the spots in the sliver sample gave an yellow coloration with red edges. At the same height, the authentic NG sample was also noticed. The plate was sprayed with titanous chloride/p-dimethyl amino benzaldehyde for the identification of DNT and TNT. A reddish color spot was observed on the sliver sample, indicating the presence of DNT and TNT. Tests were carried out for the identification of 2nDPA and its derivatives with saturated alcoholic KOH and from the coloration of these spots, the derivatives were identified. These results of the TLC analysis indicate the presence of all the ingredients, together with derivatives of 2-nDPA.

The sliver residue was subjected to differential scanning calorimetric (DSC) analysis. The DSC (Perkin-Elmer DSC-28) experiments were carried out according to the manufacturer's instructions. The quantity of the sample taken for the analysis was around 3 mg. The DSC thermogram of the sliver sample was recorded in N_2 (30 ml/min) at a heating rate of 16°C/min. The thermogram of sliver and propellant powder are shown in Fig. 1.

Results and Discussion

The DSC results are presented in Table 1, which shows that the heat of decomposition for the sliver residue is much less than that of the propellant powder. The TLC of sliver residue indicated the presence of NG, DNT, and/or TNT and 2-nDPA and its derivatives. The results of these experiments are of only a qualitative nature. The heats of decomposition (ΔH) for the sliver residue, propellant powder, NG, DNT, and 2-nDPA were obtained experimentally using DSC analysis. The values are presented in Table 1. It may be seen that the ΔH of the NC is much higher than that of a propellant. For all other major propellant ingredients, the heat of decomposition is endothermic. This means that the exothermicity of propellant decomposition is mostly due to NC. The heat of decomposition of the sliver residue is seen to be less than that of the propellant powder. The decrease in the heat of decomposition indicates that the sliver residue is depleted with NC.

Table 1 Thermal decomposition data

Sliver No.	Component	Heat of decomposition, cal/g
1	Propellant power	−210
2	Sliver residue	−90.5
3	Propellant (block)	−156.0
4	Nitrocellulose	−336
5	Nitroglycerine	+47.3
6	Dinitro toluene	+118.8
7	Trinitro toluene	+163.0

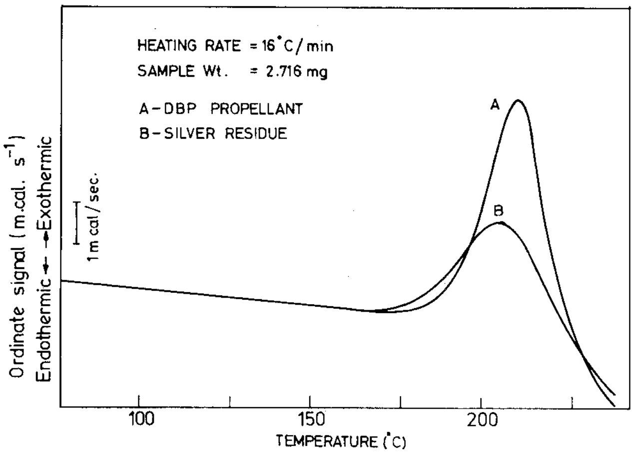

Fig. 1 DSC thermograms of DBP propellant and its sliver residue.

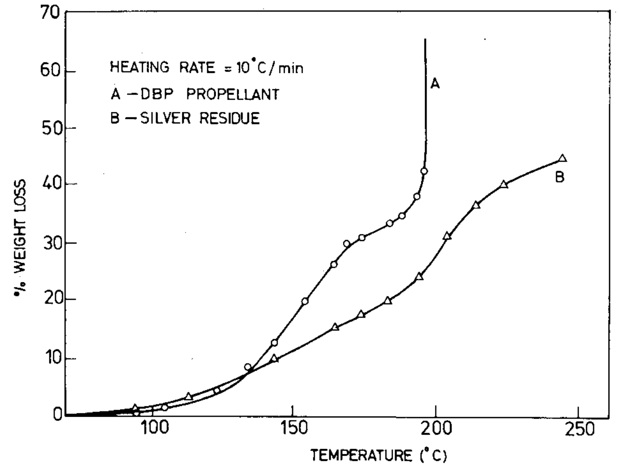

Fig. 2 TG trace of DBP propellant and its silver residue.

Thermogravimetry (TG) results are shown in Fig. 2, which shows that the weight loss rate and the extent of the weight loss in the sliver residue are much less than those in the original propellant. The TG curve for the propellant is comparable with earlier work.[3] Around 195°C, there is a sudden weight loss (knee) in the propellant that corresponds to the NC decomposition; at the same heating rate, NC decomposition shows a knee at the same temperature. In the sliver residue, this knee is not seen; instead, a slow weight loss is noticed, indicating either that the percentage of NC may be less or that the NC may be degraded. In order to confirm the DSC and TG results that the NC is depleted in the sliver residue, the sliver residue and propellant powder were subjected to gravimetric estimations. Known weights of the sliver residue and the propellant powder were dissolved in dichloromethane. The samples were subjected to Soxhlet extraction for 8 h with the same solvent. The samples were removed and dried. The insoluble matter was weighed and the percentage weight loss was determined. There was 69% insoluble matter in the propellant powder. The insoluble matter in both samples was made up of NC and inorganic salts. Inorganic salt in the propellant accounts maximum of only 3.5%. These results clearly indicate that the sliver residue is depleted with NC, which means that the sliver surface is rich with NG. The presence of NG was also confirmed by TLC analysis. This observation shows that during the combustion process the surface layer (to a certain depth) contains a considerable amount of NG.

Scanning electron microscopy photographs of the sliver surface showed crests and cavities of an irregular size and shape. It is believed that a bubble is formed in a cavity at a solid surface due to liquid, which suggests that boiling is occurring within the surface. This may be due to the fact that the NG and volatiles liquify first in these cavities and that the bubble formation takes place inside the propellant matrix. After growing to a certain critical size, these bubbles burst out from the surface. This observation supports the fact that the surface is richer in NG.

The fact the burning surface is rich with NG and is depleted of NC implies that on the surface the NC decomposes first. Carbon was found to be a residue at the end of the thermal decomposition of NC and DBP, which suggests that the exothermic decomposition of NC gives off products such as solid carbon along with the gaseous ones. This may be the reason for the observation of carbon particles on the burning surface by Heath and Hirst.[4] They also observed a number of globules on the surface that they attributed to gas bubbles. These globules may be NG and other volatile components of DBP leaving the surface.

In view of the above discussion, it is appropriate to say that NC first decomposes on the surface exothermically and NG boils, vaporizes, and finally diffuses out of the surface. The decomposition of NC is too fast and hence cannot control the surface regression reactions. It is likely that NG diffusion, being the slower step, may be the rate-controlling step. These decomposed products of NC and the vaporized NG along with other volatiles may react and produce heat in the fizz zone.

Conclusions

The large amount of heat required for double-base propellant regression may be caused by the exothermic heat released during NC decomposition in the condensed phase.

During low-temperature decomposition of the DBP, NG undergoes diffusional vaporization and leaves behind a decomposed propellant richer in NC.[5] On the other hand, during burning NC decomposes and leaves the burning surface richer in NG. It may be said that since NC primarily governs the propellant regression, burning rate modifications could be effectively carried out by those methods that bring about changes in the thermal decomposition behavior of NC.

References

[1] Kishore, K., Pai Verneker, V. R., Chaturvedi, B. K., and Gayathri, V., "Mechanistic Studies on Composite Solid Propellants," *AIAA Journal*, Vol. 15, Jan. 1977, pp. 114-116.

[2] Kishore, K., Pai Verneker, V. R., and Gayathri, V., "Reaction Intermediates during Combustion and Decomposition of Some Model Solid Rocket Fuels," *Fuel*, Vol. 60, Feb. 1981, pp. 164-167.

[3] Pai Verneker, V. R., Kishore, K., and Subhas, C.B.V., "Thermal Reactivity of Double Base Rocket Propellants," *Propellants and Explosives*, Vol. 4, 1979, pp. 83-86.

[4] Heath, G. A. and Hirst, R., "Some Characteristics of the High Pressure Combustion of Double-Base Propellants," *Eighth Symposium (International) on Combustion*, Williams and Wilkins Co., Baltimore, Md., 1960, pp. 711-719.

[5] Pai Verneker, V. R., Kishore, K., and Subhas, C.B.V., "Comparative Assessment of the Thermal Decomposition and Combustion Behavior in Double Base and Composite Solid Propellants," *AIAA Journal*, to be published.

Stability of Annular Sector Plates with Variable Thickness

R. S. Srinivasan* and V. Thiruvenkatachari†
Indian Institute of Technology, Madras, India

Introduction

ALTHOUGH many researchers have studied the buckling of circular and annular plates, the only reference available on the stability of annular sector plates is that of Rubin.[1] Rubin has considered a plate with simply supported radial edges with arbitrary boundary conditions along curved edges. The plate is subjected to constant in-plane forces along the radial and circumferential directions.

In this Note the stability analysis of a clamped annular sector plate with variable thickness subjected to uniform load along the radial direction is presented. A numerical method using matrix algebra, which had been adopted earlier for the study of buckling of skew plates,[2] has been used.

Differential Equations

Consideration of the equilibrium of the plate shown in Fig. 1 results in

$$\frac{\partial}{\partial r}(rM_r)+\frac{\partial}{\partial\theta}(M_{r\theta})-M_\theta-rQ_r=0 \tag{1}$$

$$\frac{\partial}{\partial r}(rM_{r\theta})+\frac{\partial}{\partial\theta}(M_\theta)+M_{r\theta}-rQ_\theta=0 \tag{2}$$

$$\frac{\partial}{\partial r}\left[rN_r\frac{\partial w}{\partial r}+N_{r\theta}\frac{\partial w}{\partial\theta}+rQ_r\right]+\frac{\partial}{\partial\theta}\left[\frac{1}{r}N_\theta\frac{\partial w}{\partial\theta}+N_{r\theta}\frac{\partial w}{\partial\theta}+Q_\theta\right]=0 \tag{3}$$

$$\frac{\partial}{\partial r}(rN_r)+\frac{\partial}{\partial\theta}(N_{r\theta})-N_\theta=0 \tag{4}$$

$$\frac{\partial}{\partial r}(rN_{r\theta})+\frac{\partial}{\partial\theta}(N_\theta)+N_{r\theta}=0 \tag{5}$$

The boundary conditions are

at

$$r=a,\quad N_r=\frac{P}{a\theta_0},\quad N_{r\theta}=w=\frac{\partial w}{\partial r}=0 \tag{6a}$$

$$r=b,\quad N_r=\frac{P}{b\theta_0},\quad N_{r\theta}=w=\frac{\partial w}{\partial r}=0 \tag{6b}$$

$$\theta=0 \text{ and } \theta_0,\quad N_\theta=N_{r\theta}=w=\frac{\partial w}{\partial\theta}=0 \tag{6c}$$

where P is the total load applied uniformly on a curved edge.

The solution of Eqs. (4) and (5) subjected to the in-plane boundary condition mentioned in Eqs. (6) can be written from Ref. 3 as

$$N_r=-\frac{2P\cos(-\theta_0/2+\theta)}{r(\theta_0+\sin\theta_0)},\quad N_\theta=N_{r\theta}=0 \tag{7}$$

Using Eqs. (1-3) and noting that the rigidity of the plate is not constant, the governing differential equation can be written as

$$\nabla^2(D\nabla^2 w)-(1-\mu)\left[\frac{\partial^2 D}{\partial r^2}\left(\frac{1}{r}\frac{\partial w}{\partial r}+\frac{1}{r^2}\frac{\partial^2 w}{\partial\theta^2}\right)-2\frac{\partial}{\partial r}\left(\frac{1}{r}\frac{\partial D}{\partial\theta}\right)\times\frac{\partial}{\partial r}\left(\frac{1}{r}\frac{\partial w}{\partial\theta}\right)+\frac{\partial^2 w}{\partial r^2}\left(\frac{1}{r}\frac{\partial D}{\partial r}+\frac{1}{r^2}\frac{\partial^2 D}{\partial\theta^2}\right)\right]=N_r\frac{\partial^2 w}{\partial r^2} \tag{8}$$

where

$$\nabla^2=\left(\frac{\partial^2}{\partial r^2}+\frac{1}{r}\frac{\partial}{\partial r}+\frac{1}{r^2}\frac{\partial^2}{\partial\theta^2}\right)$$

and

$$D=\frac{Eh^3}{12(1-\mu^2)}$$

and μ is Poisson's ratio.

Taking the thickness variation as (see Fig. 1)

$$h=h_0\{1+[\bar{r}-(b/c)]\eta\}=h_0H(\bar{r}) \tag{9}$$

Received Nov. 29, 1982.

*Professor, Department of Applied Mechanics.

†Research Scholar, Department of Applied Mechanics.